29th Nordic Seminar on Computational Mechanics
NSCM-29
R. Larsson (Ed.)
2016

MODELLING OF IG-SCC MECHANISM THROUGH COUPLING OF A POTENTIAL-BASED COHESIVE MODEL AND FICK'S SECOND LAW

M. SEDLAK*, B. ALFREDSSON* AND P. EFSING*

*Department of Solid Mechanics
Royal Institute of Technology, KTH
100 44 Stockholm, Sweden

Key words: Multi-physics, Cohesive element, Crack growth, Corrosion.

Summary. A model has been developed to predict crack growth velocities in IG-SCC, at stress and ion variation. The model is a coupling between Fick's second law and a newly developed cohesive element with degradation of damage resisting properties, implemented into a user element in ABAQUS. High stresses at the crack tip are assumed to drive the corrosion process and change the diffusivity. The stress and ion concentrations are varied which shows that higher stresses or higher ion concentrations gives thicker oxides and higher crack propagation velocities.

1 INTRODUCTION

The current trend for extended life of many Nuclear Power Plants is to extend beyond the originally planned operation time. The extended service time makes it increasingly important to understand the ageing processes of materials[1]. Intergranular Stress Corrosion Cracking (IG-SCC) is one of the most commonly recognized degradation phenomena. From a phenomenological view it is well-known and has been investigated for a long time but due to its complicated nature it is still not completely understood. In particular a coupled mechanic and corrosion model is for the degradation process. Earlier research on IG-SCC mostly focused on identifying the material and corrosion behavior trough experiments and parameter fitting equations[2,3]. The currently presented work is based on a multi-physics model, created to mimic one of the more accepted mechanisms of IG-SCC[4]. In which the exposure to water allows oxides to penetrate along grain boundaries (the rate is governed by strain, time, ion concentration etc.). The oxide weakens the mechanical strength of the grain boundaries and the boundaries will eventually crack due to the applied stress leaving new virgin material exposed. This process will repeat itself and cracks will grow continuously, see Figure 1a.

2 Model

The model is based on the coupling between the equilibrium equation and the diffusion equation. This coupled equations are inserted into an FE cohesive element[5,6]. The equilibrium equation is coupled with the diffusion equation

$$\frac{\partial c}{\partial t} = D(\eta_T)\frac{\partial^2 c}{\partial x^2} - h(c, \eta_T^{rev}) \tag{1}$$

where $D(\eta_T)$ is the diffusivity as a function of irreversible normalized traction $\eta_T[1,0]$, c is the concentration of ions and $h(c, \eta_T^{rev})$ is the adsorption rate of the ions to the boundaries, i.e. the crack and crack tip faces. The crack mouth has the boundary condition (BC) of constant concentration, no other BC is applied, see Figure 1b. The diffusion model in Equation 1 describes the transport of ions from the crack mouth to the crack tip. In Fick's second law the cross section area and length is influencing the diffusion, meaning that longer travel distances will experience more concentration loss. The diffusivity is defined as

$$D(\eta_T) = (D_s - D_l)\eta_T + D_l \tag{2}$$

where the diffusivity function $D(\eta_T)$ has the requirement to change from the diffusivity of the ions in the undamaged grain boundary material D_s to the diffusivity of the ions in the liquid D_l. A simple definition of $h(c, \eta_t^{rev})$ was assumed

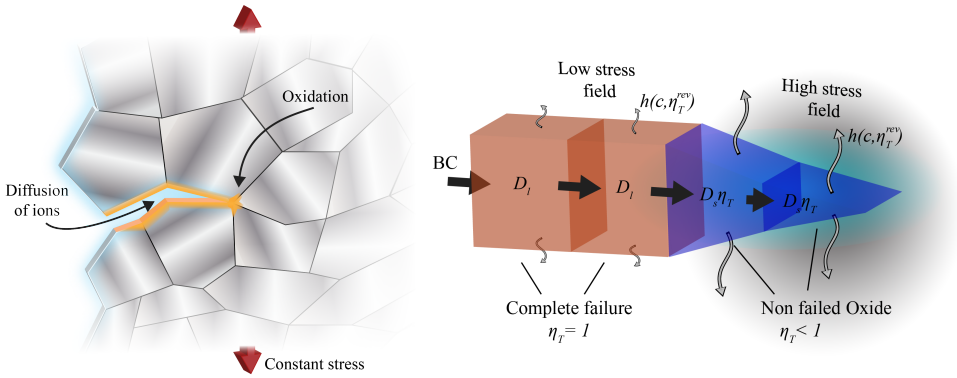

(a) (b)

Figure 1: (a) Ions diffusing inside the crack tip create oxides on the crack walls and at crack tip. Constant far field stress promotes the process. (b) Schematic figure showing ions passing through the crack from the mouth to the tip by diffusion. The red elements represent failed elements while the blue elements are not yet failed (with different diffusivity).

$$h(c, \eta_T^{rev}) = \dot{c}^{\,max}\left(1 - \exp(-n_1(\eta_T^{rev})c)\right) \tag{3}$$

where $\dot{c}^{max}$ is the maximum adsorption rate and $n_1(\eta_T^{rev})$ is a function depending on the reversible normalized traction, which is changing the angle of the exponential slope resulting in a different adsorption velocity at specific ion concentrations.

2.1 Degradation implementation

The oxides fracture properties are obtained by changing the Traction Separation Law (TSL) of the cohesive element. The fracture energy ϕ is controlled by the amount of oxidation, which in its turn is linked to the amount of ions adsorbed at the surface

$$\phi \propto \int h(c)dt = c^{ad} \tag{4}$$

The relation between the fracture energy and the amount of ions is assumed to be linear using $k^{\phi}_{c^{ad}}[> 0, \infty)]$. It is subtracted from the initial energy ϕ^{ini}

$$\phi = \phi^{ini} - k^{\phi}_{c^{ad}} c^{ad} \tag{5}$$

where the oxide fracture energy is a minimum limit and the initial energy is a maximum limit $\phi[\phi_{oxd}, \phi_{ini}]$,

3 Applications to DCB specimen

The double cantilever beam (DCB) was used to test the multi-physics cohesive elements. The DCB is constrained at the bottom node of the cracked side of the specimen and a constant force is applied to the corresponding upper node. The model is force controlled and the geometric dimension for the DCB model is $a = 5$ μm, $L = 10$ μm and $b = 2$ μm. The fracture energy is $\phi = 20$ J/ μm^2 and the maximum cohesive traction is $T_n^{ini} = 0.2$ MPa. The bulk elements are elastic with the Young's modulus $E = 200$ GPa and the Poisson's ratio $\nu = 0.3$. The energy for the oxide material is reduced to half of the initial traction and a tenth of the fracture energy. Figure 2a shows the oxide start and crack tip position for the simulated crack growth. The thickness of the degrading oxide is the distance along the grain boundary where the element is not completely damage yet but has adsorbed ion. The oxide thickness is obtained from Figure 2a as the vertical distance between the two curves. The oxide thickness is constant except for the start of the computation. Figure 2b presents the velocity for the oxide start and crack tip. The stress and ion concentration are varied in the simulations with results in Figure 3a and 3b. As expected higher stresses or higher ion concentrations gives thicker oxides.

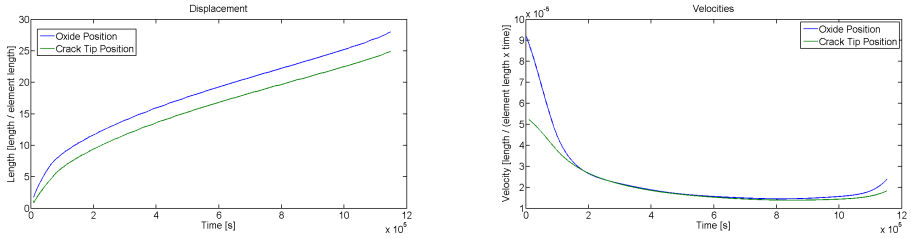

(a) (b)

Figure 2: (a) Crack tip and the oxide start positions for the growing crack. (b) Velocity of the growing crack tip and the oxide start position.

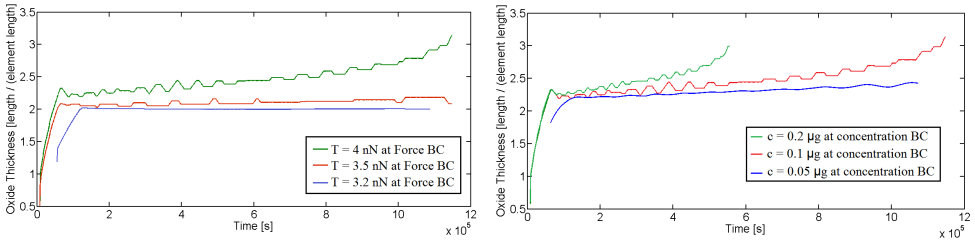

(a) (b)

Figure 3: (a) Influence of stress level on the oxide thickness. (b) Oxide thickness for some different ion concentrations.

REFERENCES

[1] Öijerholm, J. & Jenssen, A. Interkristallin spänningskorrosion i rostfritt stål i BWR-miljö – En sammanställning av kunskapsläget med fokus på\: erfarenheter av studier genomförda i Sverige (2015).

[2] Smith, T. & Staehle, R. Role of Slip Step Emergence in the Early Stages of Stress Corrosion Cracking in Face Centerd Iron-Nickel-Chromium Alloys. *Corrosion* **23**, 117–129 (1967).

[3] Parkins, R. N. Predictive approaches to stress corrosion cracking failure. *Corrosion Science* **20**, 147–166 (1980).

[4] Ford, F. P. Quantitative Prediction of Environmentally Assisted Cracking. *Corrosion* **52**, 375–395 (1996).

[5] Barenblatt, G. The Mathematical Theory of Equilibrium Cracks in Brittle Fracture. In *Advances in Applied Mechanics*, vol. 7, 55–129 (1962).

[6] Dugdale, D. Yielding of steel sheets containing slits. *Journal of the Mechanics and Physics of Solids* **8**, 100–104 (1960).